SCATTERING AND EMISSIVITIES OF OBLIQUE INCIDENT WAVES FROM DOUBLE-LAYERED RANDOM ROUGH SURFACES IN REMOTE SENSING OF SNOW

Peng Xu[1] *and Jian-Cheng Shi*[2]

[1]School of Electronic Information, Wuhan University, Wuhan 430072, China
[2]The Institute of Remote Sensing Applications of Chinese Academy of Sciences, Beijing 100101, China

pxu@whu.edu.cn

ABSTRACT

In this paper it is studied for 2-D scattering and emissivities of oblique incident waves from double-layered random rough surfaces. At oblique incidence, the cross-polarization scattering is presented for double-layered snow surfaces with large heights and large slopes. Numerical results show that the cross-polarization results can be large to degree of those of co-polarization at a large oblique incident angle. All four Stokes parameters are also calculated for polarimetric passive remote sensing of snow layered media. The Stokes parameters presented in this paper are compared with the previously published results with periodic boundary condition, and the artificial kinks and abruptions imposed by Floquet models are removed in this new model.

Index Terms— random rough surface, scattering, emissivity, microwave remote sensing

1. INTRODUCTION

Active and passive microwave remote sensing have been applied to terrestrial snow. The remote sensing is important as the microwave signatures yield information of the physical parameters of the snow. By observing the changes in the physical parameters over time, inter-annual changes across some snow place can be monitored. Understanding the changes of the snow surface can be related to global climate change. An empirical model is used to parameterize the scattering signature over ice sheets. The model parameters are empirical parameters rather than physical parameters. Interpretation of passive microwave measurements of SSM/I over Greenland have also been made using a layered model of snow and ice [1].

The changes in the radar cross section can be related to snow melt and to changes in accumulation. Ashcraft and Long [2] were also able to demonstrate strong azimuth dependence of the backscattering signatures by examining the radar cross section as a function of azimuthal angle for a range of azimuthal angles. The azimuth angle dependence can be used to relate to the surface profiles particularly to the wind-formed erosion features known as sastrugi. Sastrugi crests are parallel to the wind direction.

Kuo *et al*. [3] and Liang *et al*. [4] examed the scattering of normal incident waves from multilayer random rough surfaces in the context with co-polarizations. Johnson *et al*. [5] used double-layered model to study passive polarimetry of wind direction over the ocean. However, their results did not exhibit the large fourth Stokes parameter. In 2008 Tsang *et al.* [6] proposed a model of anisotropic periodic rough surfaces with large slopes and large heights over layered media, which showed the possibility of large fourth Stokes parameter. Xu *et al.* [7] showed that the model of two-layer periodic rough surface could also produce large fourth Stokes parameter even for case of small slopes. Later Chang and Tsang [8] extended the work of Liang *et al*. [4] to the 3D problem by random Sastrugi surfaces over multilayers, thus they eliminated angular fluctuations of four Stokes parameters.

Most natural surfaces are generally not smooth but random rough. In this paper, different from the previous model in ref. [7], where the two rough surfaces are both periodic, and also different from one in ref. [8], where only the top interface is random rough while the others are all flat faces, a double-layered random rough surface is studied to simulate the bistatic scattering for both co-polarizations and cross-polarizations in active microwave remote sensing, and all four Stokes parameters in passive microwave remote sensing. We use the surface integral equation approach to treat 3D scattering, emission and absorption of a double-layered random rough surface. Numerical results are illustrated for polarimetric microwave remote sensing.

2. METHODLOGY

As shown in Fig. 1, consider a plane wave incident upon a double-layered random rough surface with height profile $z = f_1(x)$ and $z = f_2(x)$ with f_1 and f_2 representing the top and the bottom surfaces, respectively. The second rough surface is placed at $z = -d$ below the top one. The

978-1-4673-5225-3/14/$31.00 ©2014 IEEE

region zero above the top surface is air, the other two layers are with permittivities of ε_1 and ε_2, respectively.

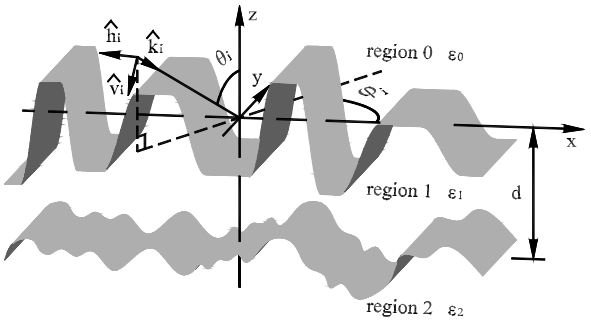

Fig. 1 Geometry of a double-layered random rough surface.

The incident electromagnetic fields are given by

$$\begin{cases} \overline{E}_i = E_{vi}\hat{v}_i + E_{hi}\hat{h}_i & (1a) \\ \eta\overline{H}_i = E_{vi}\hat{h}_i - E_{hi}\hat{v}_i & (1b) \end{cases}$$

where

$$\begin{cases} \hat{k}_i = \sin\theta_i\cos\phi_i\hat{x} + \sin\theta_i\sin\phi_i\hat{y} - \cos\theta_i\hat{z} & \\ \hat{h}_i = -\sin\phi_i\hat{x} + \cos\phi_i\hat{y} & (2a) \\ \hat{v}_i = -\cos\theta_i\cos\phi_i\hat{x} - \cos\theta_i\sin\phi_i\hat{y} - \sin\theta_i\hat{z} & (2b) \\ & (2c) \end{cases}$$

$$\begin{cases} E_{hi} = \cos\alpha\psi_{\text{inc}}\exp(-i\beta) & (3a) \\ E_{vi} = \sin\alpha\psi_{\text{inc}} & (3b) \end{cases}$$

where $k_{ix} = k\sin\theta_i\cos\phi_i$; $k_{iy} = k\sin\theta_i\sin\phi_i$; $k_{iz} = k\cos\theta_i$.

The surface integral equations based on Maxwell's equations with the boundary conditions can be discretized by MoM with rooftop basis functions and Galerkin's method, and result in a following matrix equation of dimensions $8N\times 8N$.

$$\begin{bmatrix} a_1\overline{\overline{A}}^{(1)}_{(s_0,s'_0)} & \overline{\overline{B}}^{(1)}_{(s_0,s'_0)}\overline{\Delta}_{0n} & c_1\overline{\overline{C}}^{(1)}_{(s_0,s'_0)}\overline{\Delta}_{0n} & 0 & -\overline{\overline{A}}^{(1)}_{(s_0,s'_1)} & -\overline{\overline{B}}^{(1)}_{(s_0,s'_1)}\overline{\Delta}_{1n} & 0 & 0 \\ \overline{\overline{A}}^{(0)} & \overline{\overline{B}}^{(0)}\overline{\Delta}_{0n} & 0 & 0 & 0 & 0 & 0 & 0 \\ 0 & 0 & \overline{\overline{B}}^{(0)}\overline{\Delta}_{0n} & \overline{\overline{A}}^{(0)} & 0 & 0 & 0 & 0 \\ 0 & -\tau_1 c_1\overline{\overline{C}}^{(1)}_{(s_0,s'_0)}\overline{\Delta}_{0n} & \overline{\overline{B}}^{(1)}_{(s_0,s'_0)}\overline{\Delta}_{0n} & \tau_1 a_1\overline{\overline{A}}^{(1)}_{(s_0,s'_0)} & 0 & 0 & -\sqrt{\tau_1}\overline{\overline{B}}^{(1)}_{(s_0,s'_1)}\overline{\Delta}_{1n} & -\sqrt{\tau_1}\overline{\overline{A}}^{(1)}_{(s_0,s'_1)} \\ 0 & 0 & 0 & 0 & a_2\overline{\overline{A}}^{(2)}_{(s_1,s'_1)} & \overline{\overline{B}}^{(2)}_{(s_1,s'_1)}\overline{\Delta}_{1n} & c_2\overline{\overline{C}}^{(2)}_{(s_1,s'_1)}\overline{\Delta}_{1n} & 0 \\ -a_1\overline{\overline{A}}^{(1)}_{(s_1,s'_0)} & -\overline{\overline{B}}^{(1)}_{(s_1,s'_0)}\overline{\Delta}_{0n} & -c_1\overline{\overline{C}}^{(1)}_{(s_1,s'_0)}\overline{\Delta}_{0n} & 0 & \overline{\overline{A}}^{(1)}_{(s_1,s'_1)} & \overline{\overline{B}}^{(1)}_{(s_1,s'_1)}\overline{\Delta}_{1n} & 0 & 0 \\ 0 & \tau_1 c_1\overline{\overline{C}}^{(1)}_{(s_1,s'_0)}\overline{\Delta}_{0n} & -\overline{\overline{B}}^{(1)}_{(s_1,s'_0)}\overline{\Delta}_{0n} & -\tau_1 a_1\overline{\overline{A}}^{(1)}_{(s_1,s'_0)} & 0 & 0 & \sqrt{\tau_1}\overline{\overline{B}}^{(1)}_{(s_1,s'_1)}\overline{\Delta}_{1n} & \sqrt{\tau_1}\overline{\overline{A}}^{(1)}_{(s_1,s'_1)} \\ 0 & 0 & 0 & 0 & 0 & -\tau_2 c_2\overline{\overline{C}}^{(2)}_{(s_1,s'_1)}\overline{\Delta}_{1n} & \overline{\overline{B}}^{(2)}_{(s_1,s'_1)}\overline{\Delta}_{1n} & \tau_2 a_2\overline{\overline{A}}^{(2)}_{(s_1,s'_1)} \end{bmatrix} \begin{bmatrix} \overline{\Delta\ell}_0\overline{\chi}_0 \\ \overline{\psi}_0 \\ \eta\overline{\varphi}_0 \\ \overline{\Delta\ell}_0\eta\overline{\xi}_0 \\ \overline{\Delta\ell}_1\overline{\chi}_1 \\ \overline{\psi}_1 \\ \eta_1\overline{\varphi}_1 \\ \overline{\Delta\ell}_1\eta_1\overline{\xi}_1 \end{bmatrix} = \begin{bmatrix} \overline{0} \\ \overline{E}_{iyw} \\ \eta\overline{H}_{iyw} \\ \overline{0} \\ \overline{0} \\ \overline{0} \\ \overline{0} \\ \overline{0} \end{bmatrix} \quad (4)$$

The bistatic scattering coefficients of θ_s, φ_s in terms of Θ_s

$$\begin{cases} \sigma_{h\Lambda}(\Theta_s) = \dfrac{k}{16\pi\eta k_t^2 P_{\text{inc}}}\dfrac{\left|k\sin\Theta_s e^s_{yw}(\Theta_s) - k_{iy}\cos\Theta_s\eta h^s_{yw}(\Theta_s)\right|^2}{k^2\sin^2\Theta_s + k_{iy}^2\cos^2\Theta_s} & (5a) \\ \sigma_{v\Lambda}(\Theta_s) = \dfrac{k}{16\pi\eta k_t^2 P_{\text{inc}}}\dfrac{\left|k\sin\Theta_s\eta h^s_{yw}(\Theta_s) + k_{iy}\cos\Theta_s e^s_{yw}(\Theta_s)\right|^2}{k^2\sin^2\Theta_s + k_{iy}^2\cos^2\Theta_s} & (5b) \end{cases}$$

$$\begin{cases} \sigma^{\text{total}}_{\Lambda}(\Theta_s) = \sigma_{h\Lambda} + \sigma_{v\Lambda} = \dfrac{k}{16\pi\eta k_t^2 P_{\text{inc}}}\left(\left|e^s_{yw}(\Theta_s)\right|^2 + \left|\eta h^s_{yw}(\Theta_s)\right|^2\right) & (6a) \\ \gamma^{\text{total}}_{\Lambda}(\Theta_s) = 2\pi\sigma^{\text{total}}_{\Lambda}(\Theta_s) = \dfrac{k}{8\eta k_t^2 P_{\text{inc}}}\left(\left|e^s_{yw}(\Theta_s)\right|^2 + \left|\eta h^s_{yw}(\Theta_s)\right|^2\right) & (6b) \end{cases}$$

where $\Lambda = h,\ v$, and

$$\begin{matrix} e^s_{yw}(\Theta_s) = \\ e^s_{yw}(\theta_s,\varphi_s) \end{matrix}\Bigg\} = \begin{cases} \displaystyle\int_{s_1} dx'\frac{\psi(x')ik(f_{x'}\sin\theta_s\cos\varphi_s - \cos\theta_s) - \chi(x')}{\exp\left[ik(x'\sin\theta_s\cos\varphi_s + f_1(x')\cos\theta_s)\right]} \\ \displaystyle = \int_{s_1} dx'\frac{\psi(x')ik_t(f_{x'}\sin\Theta_s - \cos\Theta_s) - \chi(x')}{\exp\left[ik_t(x'\sin\Theta_s + f_1(x')\cos\Theta_s)\right]} \end{cases} \quad (7a)$$

$$\begin{matrix} h^s_{yw}(\Theta_s) = \\ h^s_{yw}(\theta_s,\varphi_s) \end{matrix}\Bigg\} = \begin{cases} \displaystyle\int_{s_1} dx'\frac{\phi(x')ik(f_{x'}\sin\theta_s\cos\varphi_s - \cos\theta_s) - \xi(x')}{\exp\left[ik(x'\sin\theta_s\cos\varphi_s + f_1(x')\cos\theta_s)\right]} \\ \displaystyle = \int_{s_1} dx'\frac{\phi(x')ik_t(f_{x'}\sin\Theta_s - \cos\Theta_s) - \xi(x')}{\exp\left[ik_t(x'\sin\Theta_s + f_1(x')\cos\Theta_s)\right]} \end{cases} \quad (7b)$$

$$-90^\circ \le \Theta_s \le 90^\circ \quad (8a)$$

$$\hat{\rho}_s = \sin\Theta_s\hat{x} + \cos\Theta_s\hat{z} \quad (8b)$$

$$\begin{aligned} k_s &= k_t\hat{\rho}_s + k_{iy}\hat{y} = k_t\sin\Theta_s\hat{x} + k_{iy}\hat{y} + k_t\cos\Theta_s\hat{z} \\ &= k\left(\sin\theta_s\cos\varphi_s\hat{x} + \sin\theta_i\sin\varphi_i\hat{y} + \cos\theta_s\hat{z}\right) \end{aligned} \quad (8c)$$

Emissivity is equal to absorptivity. After the surface fields are determined, absorptivity and reflectivity can be calculated by

$$\begin{cases} a(\theta_i,\varphi_i) = +\dfrac{k}{k_t^2 P_{\text{inc}}}\operatorname{Im}\displaystyle\int_{s_1} dx\left[\psi(x)\chi^*(x) - \eta^2\xi(x)\phi^*(x)\right] & (9a) \\ r(\theta_i,\varphi_i) = -\dfrac{k}{k_t^2 P_{\text{inc}}}\operatorname{Im}\displaystyle\int_{s_1} dx\left[\psi^s(x)\chi^{s*}(x) - \eta_0^2\xi^s(x)\phi^{s*}(x)\right] & (9b) \end{cases}$$

The Energy conservation check is performed by verifying that $r(\theta_i,\varphi_i) + a(\theta_i,\varphi_i) = 1$.

For polarizations, let $\mathrm{v}, \mathrm{h}, +45^\circ, -45^\circ, \mathrm{LC}, \mathrm{RC}$ be vertical, horizontal, $+45^\circ$ linear, -45° linear, left-hand circular and right-hand circular polarizations respectively. The brightness temperatures are related to the emissivities by

$$\mathrm{T}(\theta_i,\varphi_i) = e(\theta_i,\varphi_i)\mathrm{T}_0 \quad (10)$$

where T_0 is the physical temperature. The four Stokes parameters are $\mathrm{T_v}$, $\mathrm{T_h}$, $\mathrm{U} = \mathrm{T}_{+45^\circ} - \mathrm{T}_{-45^\circ}$, and $\mathrm{V} = \mathrm{T_{LC}} - \mathrm{T_{RC}}$.

3. NUMERICL RESULTS AND DISCUSSON

In this paper, we illustrate the numerical simulation results of the bistatic scattering coefficients and the Stokes parameters for all polarizations. They are based on tapered wave approach. All energy tests conducted satisfy energy conservation to less than 1%.

The Sastrugi surface is set randomly with height 30 cm and the bottom surface is Gaussian correlated with rms of 1

cm and correlation length of 4 cm. As shown in Fig. 2, the cross-polarizations are predominant at backward while the co-polarization ones are predominant at forward direction.

However, if set $\varphi_i = 0$, the cross-polarizations disappear as shown in Fig. 3.

Seen from Fig. 4, it is also found that the internal reflections can enhance scattering dramatically.

We can also find that the internal reflections can reduce the first and second Stokes parameters remarkably as shown in Table I. On the other hand, the large third and fourth Stokes parameters shown in previously periodic structure [6, 7] disappear.

ACKNOWLEDGMENT

This work is supported in part by the National Science Foundation of China (NSFC) grant 41171291, in part by Open Fund of State Key Laboratory of Remote Sensing Science (Grant No. OFSLRSS201110).

4. REFERENCES

[1] N. C. Grody and A. N. Basist, "Interpretation of SSM/I measuremnst over Greenland", *IEEE Trans. Geosci. Remote Sens*, vol. 35, pp. 360-366, 1997.

[2] I. S. Ashcraft and D. G. Long, "Observation and Characterization of radar Backscatter over Greenland", *IEEE Trans. Geosci. Remote Sens*., vol. 43, pp. 225-237, 2005.

[3] C. H. Kuo, and M. Moghaddam, "Scattering From Multilayer Rough Surfaces Based on the Extended Boundary Condition Method and Truncated Singular Value Decomposition," *IEEE Trans. on Antennas Propaga.,* vol. 54, no. 10, pp. 2917 – 2929, 2006.

[4] D. Liang, P. Xu, L. Tsang, Z. Gui, and K. S. Chen, "Electromagnetic Scattering by Rough Surfaces with Large Heights and Slopes with Applications to Microwave Remote Sensing of Rough surface over Layered Media," *Progress In Electromagnetics Research*, PIER 95, pp. 199-218, 2009.

[5] J. T. Johnson, J. A. Kong, R. T. Shin, D. H. Staelin, K. O'Neill, and A. W. Lohanick, "Third Stokes parameter emission from a periodic water surface," *IEEE Trans. Geosci. Remote Sens*., vol. 31, no. 5, pp. 1066-1080, Sep., 1993.

[6] L. Tsang, P. Xu, and K. S. Chen, "Third and Fourth Stokes Parameters in Polarimetric Passive Microwave Remote Sensing of Rough Surfaces over Layered Media," *Microwave Opt. Technol. Lett.*, vol. 50, no. 12, pp. 3063-3069, 2008.

[7] P. Xu, L. Tsang, and K.-S. Chen, "Fourth stokes parameter in polarimetric passive remote sensing from two-layer rough surfaces," *Progress In Electromagnetics Research*, Vol. 129, 125-141, 2012.

[8] W. Chang and L. Tsang, "A partial coherent physical model of third and fourth stokes parameters of Sastrugi snow surfaces over layered media with rough surface boundary conditions of conical scattering combined with vector radiative transfer theory," *Progress In Electromagnetics Research B*, Vol. 45, 57-82, 2012.

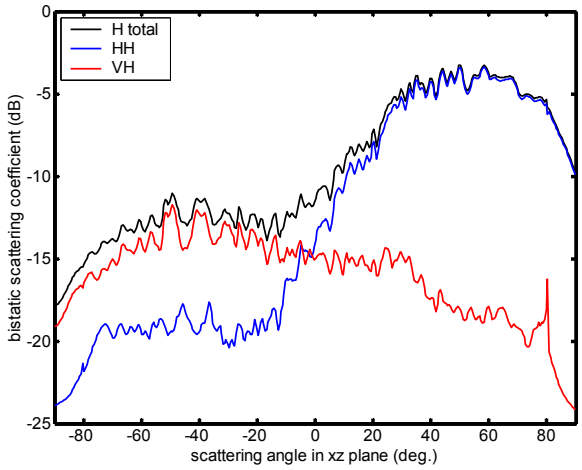

(a) Horizontal polarization incidence

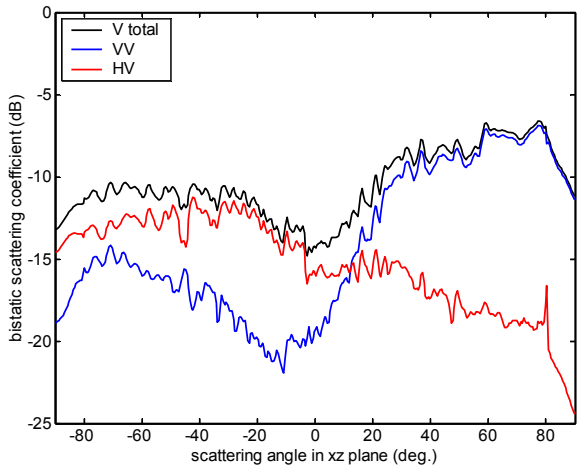

(b) Vertical polarization incidence

Fig. 2 Bistatic scattering coefficients from double-layered random rough surfaces. Top interface: Sastrugi, bottom one: Gaussian correlated surface. ε1 = 1.8, ε2 = 1.3, $\theta_i = 55°$, $\varphi_i = 45°$ and at frequency of 10.7 GHz.

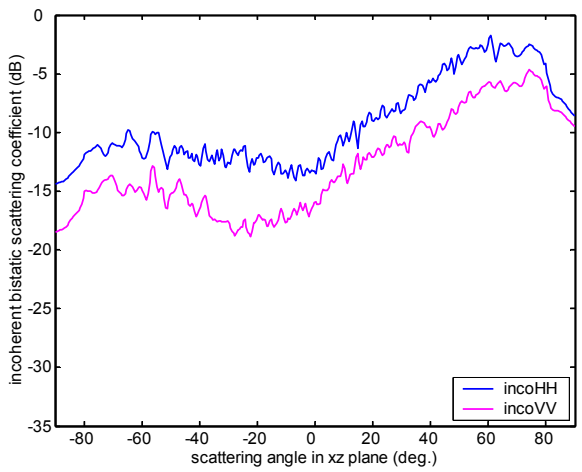

Fig. 3 Bistatic scattering coefficients with same as those in Fig. 2 except for $\varphi_i = 0$.

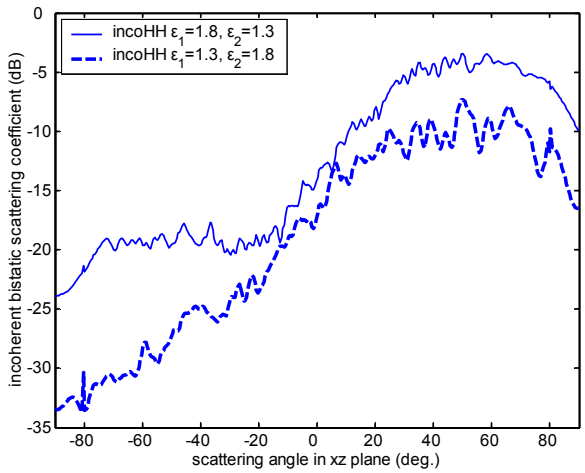

(a) For HH

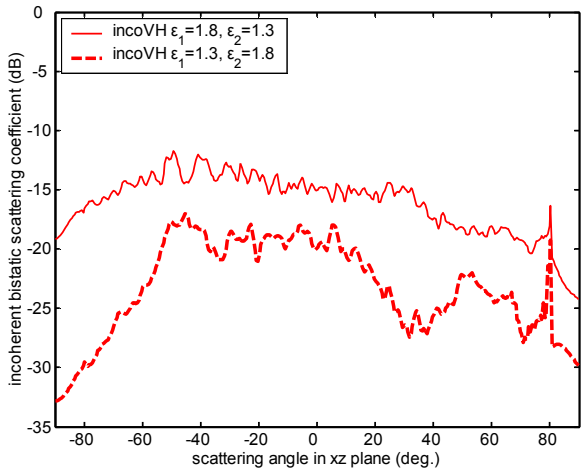

(b) For VH

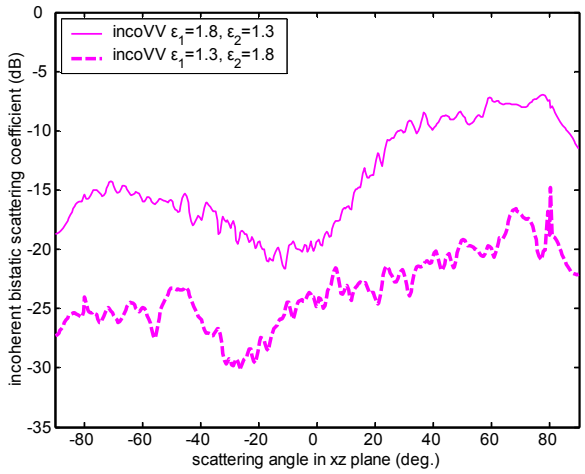

(c) For VV

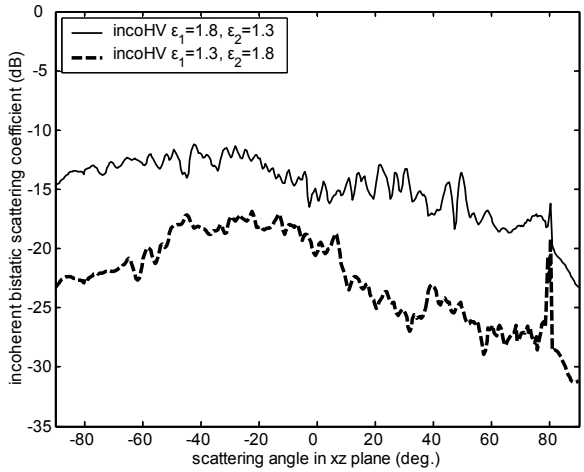

(d) For HV

Fig. 4. Comparison of bistatic scattering coefficients between with and without internal reflections. Top interface: Sastrugi, bottom one: Gaussian correlated surface. The case of ε1 = 1.8 > ε2 = 1.3 is with internal reflections while the other of ε1 = 1.3 < ε2 = 1.8 is without. $\theta_i = 55°$, $\varphi_i = 45°$ and at frequency of 10.7 GHz.

Table I Stokes parameters at some azimuthal angles

T_0=250 K	ε 1=1.8, ε 2=1.3					ε 1=1.3, ε 2=1.8		
Φ (deg.)	0	15	30	45	60		45	
Tv (K)	238.6	241.4	238.8	222.7	230.9		249.6	
Th (K)	227.0	229.3	228.9	226.8	210.7		245.4	
U (K)	0	0.01	0.01	−0.35	−0.45		−0.01	
V (K)	0	0.00	−0.01	0.10	0.10		0.00	